Received: 28 June 2019 | Revised: 19 May 2020 | Accepted: 19 May 2020

DOI: 10.1002/asl.999

Atmospheric Science Letters RMetS

RESEARCH ARTICLE

Quantifying the link between heavy precipitation and Northern Hemisphere blocking—A Lagrangian analysis

Sina Lenggenhager[1] | **Olivia Martius**[1,2]

[1]Oeschger Center for Climate Change Research and Institute of Geography, University of Bern, Bern, Switzerland

[2]Mobiliar Lab for Natural Risks, University of Bern, Bern, Switzerland

Correspondence
Sina Lenggenhager, Institute of Geography, Hallerstrasse 12, CH-3012 Bern, Switzerland.
Email: sina.lenggenhager@giub.unibe.ch

Funding information
Schweizerischer Nationalfonds zur Förderung der Wissenschaftlichen Forschung, Grant/Award Number: 156059

Abstract

Atmospheric blocks strongly influence surface weather, including extremes such as heat waves and cold spells. Recently, diabatic heating and associated upper-tropospheric potential vorticity (PV) modification have been identified as important modulators of atmospheric blocking dynamics. Also, robust links between atmospheric blocks and proximate heavy precipitation events have been established. This leads to the question of the extent to which diabatic heating associated with heavy precipitation events influences Northern Hemisphere blocking. This study uses 5 years of 3-day back trajectories started from objectively identified blocks in the ERA-Interim dataset to investigate this relationship. A substantial fraction of air parcels in blocks pass through heavy precipitation areas. The exact fraction depends on the choice of heavy precipitation threshold. Roughly 19% of all the trajectories in a block pass a heavy precipitation area (>95th percentile) area while being saturated. Of the air parcels in a block that are heated at least 5 K, 60% pass a heavy precipitation area while saturated. This fraction varies with the season and geographical area. The overall fraction is lowest in summer and highest in winter, higher over oceans than over land, and higher over the Pacific than over the Atlantic. In summer, heating is relevant over the continents and heating over North America influences blocks over the eastern Atlantic. For summer blocks in the North Atlantic and over Scandinavia, heating happens partly over the European continent.

KEYWORDS

atmospheric blocks, diabatic heating, heavy precipitation, PV modification by latent heating, trajectories

1 | INTRODUCTION

Atmospheric blocks interrupt the prevailing westerlies in the upper troposphere of the mid-latitudes. At upper levels, blocks typically consist of stationary negative potential vorticity (PV) anomalies (Illari, 1984; Schwierz *et al.*, 2004) that can be accompanied by one or more positive PV anomalies at their equatorward flanks. The flow around the block is often characterized by strong high-frequency variability (e.g., Woollings *et al.*, 2018). With a typical lifetime of a week or longer, blocks strongly impact regional weather on (sub-)seasonal time scales and are conducive to various weather extremes such as heat waves, droughts, cold spells, and floods

(e.g., Buehler *et al*., 2011; Sillmann *et al*., 2011; Sousa *et al*., 2017; Lenggenhager *et al*., 2019; Lenggenhager and Martius, 2019). Blocking modulates the occurrence of heavy precipitation events with increased frequencies of heavy precipitation upstream and partly also downstream of blocks (Lenggenhager and Martius, 2019) by altering the tracks of extratropical cyclones (Rex, 1950). A detailed case study of a flood event in Switzerland points to a potential two-way interaction between blocks and heavy precipitation events, where the latent heat release associated with heavy precipitation strengthens the upper-level negative PV anomaly of the block.

Negative upper-tropospheric PV anomalies can be generated by isentropic advection of low-PV air from regions with climatologically lower PV (i.e., from regions closer to the equator), by diabatic transport across isentropes from the lower troposphere (e.g., Hoskins *et al*., 1985; Joos and Wernli, 2012; Madonna *et al*., 2014b; Methven, 2015) or by upper-level diabatic processes related to radiative heating (Gray *et al*., 2014). PV advection is associated with synoptic-scale eddies and planetary-scale waves interacting to advect low PV into the block and with Rossby wave-breaking (Shutts, 1983; Hoskins *et al*., 1985; Nakamura *et al*., 1997; Altenhoff *et al*., 2008; Yamazaki and Itoh, 2013; Nakamura and Huang, 2017, 2018). PV advection is modulated by mid-tropospheric heating that forces upper-level irrotational winds (Grams and Archambault, 2016; Teubler and Riemer, 2016; Schneidereit *et al*., 2017; Baumgart *et al*., 2018).

The role of diabatic heating as a source of tropopause-level low PV (e.g., Madonna *et al*., 2014b; Methven, 2015) and its role in block formation has recently been recognized (e.g., Pfahl *et al*., 2015; Steinfeld and Pfahl, 2019). A climatological study of warm conveyor belts in the ERA-Interim dataset revealed significant negative PV anomalies (typically between −1 and −3 PVU) in the outflow region of warm conveyor belts in the upper troposphere. The study's authors, (Madonna *et al*., 2014b), attributed these anomalies to diabatic heating through cloud formation and precipitation during the ascent of air. These diabatically induced low PV air masses and low PV advection by irrotational winds at upper levels can have a substantial impact on the downstream development of the mid-latitude Rossby waveguide (e.g., Grams *et al*., 2011; Chagnon *et al*., 2013; Gray *et al*., 2014). Typically, the warm conveyor belt outflow, that is, the low-PV air, leads to an amplification of the downstream ridge and often to the formation of PV streamers through Rossby wave-breaking (Massacand *et al*., 2001; Madonna et al. 2014a). Both a strong ridge and the formation of PV streamers are regularly associated with the formation of blocks (e.g., Altenhoff *et al*., 2008). In addition, dynamically driven ascent associated with wave-breaking upstream of a block supports the formation of precipitation and thus latent heat release. Indeed, latent heat release and associated upper-level PV modification was found to be important for blocks (Croci-Maspoli and Davies, 2009; Pfahl *et al*., 2015; Steinfeld and Pfahl, 2019). A climatology of backward trajectories started from low-PV anomalies in blocks shows that a total of 30–45% of the air in the blocks was diabatically heated in the days before its arrival in the block (Pfahl *et al*., 2015; Steinfeld and Pfahl, 2019). A more detailed analysis shows that the enhanced divergent outflow above diabatic heating at the western flank of the block is particularly important for the stationarity of the blocks (Steinfeld and Pfahl, 2019).

In a case study, Lenggenhager *et al*. (2019) showed that air parcels that are heated during heavy precipitation events can support the formation and maintenance of downstream blocks. The aim of this paper is to further quantify the link between heavy precipitation, diabatic heating, and blocks. A strong link between heavy precipitation and blocks might be present for several reasons. First, diabatic heating in warm conveyor belts is linked to block formation. Warm conveyor belts, in turn, are strongly linked to heavy precipitation (Pfahl *et al*., 2014). In the storm track regions, warm conveyor belts drive more than 80% of 6-hourly extreme precipitation events (Pfahl *et al*., 2014). Second, diabatic heating rates are directly related to the amount of moisture that undergoes phase transitions (Joos and Wernli, 2012), so heavy precipitation is expected to be related to strong diabatic heating. This leads to the central question of this paper; namely, how frequently do air parcels that end up in blocks pass through areas of heavy precipitation prior to their arrival in the block?

Here, we extend the Lenggenhager *et al*. (2019) case study to a 5-year time period and systematically analyse the link between heavy precipitation and blocks. Specifically, we (a) quantify the fraction of air in Northern Hemispheric blocks that was strongly diabatically heated and passed over heavy precipitation areas and (b) investigate the seasonality and heating locations of diabatically heated air masses in blocks associated with heavy precipitation. In Section 2, the data, trajectory calculations, and analysis methods are introduced. The results are then presented (Section 3) and discussed (Section 4). A short summary of the main findings is presented in Section 5.

2 | DATA AND METHODS

2.1 | Reanalysis data

The ERA-Interim reanalysis dataset by the European Center for Medium Range Weather Forecast (ECMWF) (Dee

et al., 2011) for the period from 1979 to 2015 is used for all analyses. The data are interpolated onto a 1°× 1° longitude–latitude grid and is available at a temporal resolution of 6 hours. The meteorological parameters are available on 60 hybrid σ-pressure levels. As a measure for precipitation, the total daily precipitation is used, that is, the sum of snowfall, convective, and stratiform precipitation from 21 UTC the day before to 21 UTC. Extreme precipitation is defined as daily precipitation exceeding the local 95th percentile of the all-year daily precipitation accumulations, including dry days, between 1979 and 2015 (Figure 1). The local 95th percentile varies between less than 5 mm in the area of the subtropical high-pressure systems and over the Sahara to more than 25 mm over the western Pacific (Figure 1 and S1). There is also a strong seasonality in the occurrence of daily precipitation exceeding the local 95th percentile (Figure 1) that is partly due to the number of dry days per season. In winter (DJF), many extreme precipitation events occur over the eastern Pacific and the eastern Mediterranean. In spring (MAM), precipitation extremes are generally less frequent in the extra-tropics except over northern North America. In summer (JJA), precipitation extremes are frequent over Central and Eastern Europe, North Asia, and northern North America. In autumn (SON), extremes are frequent over the Pacific and the eastern Atlantic.

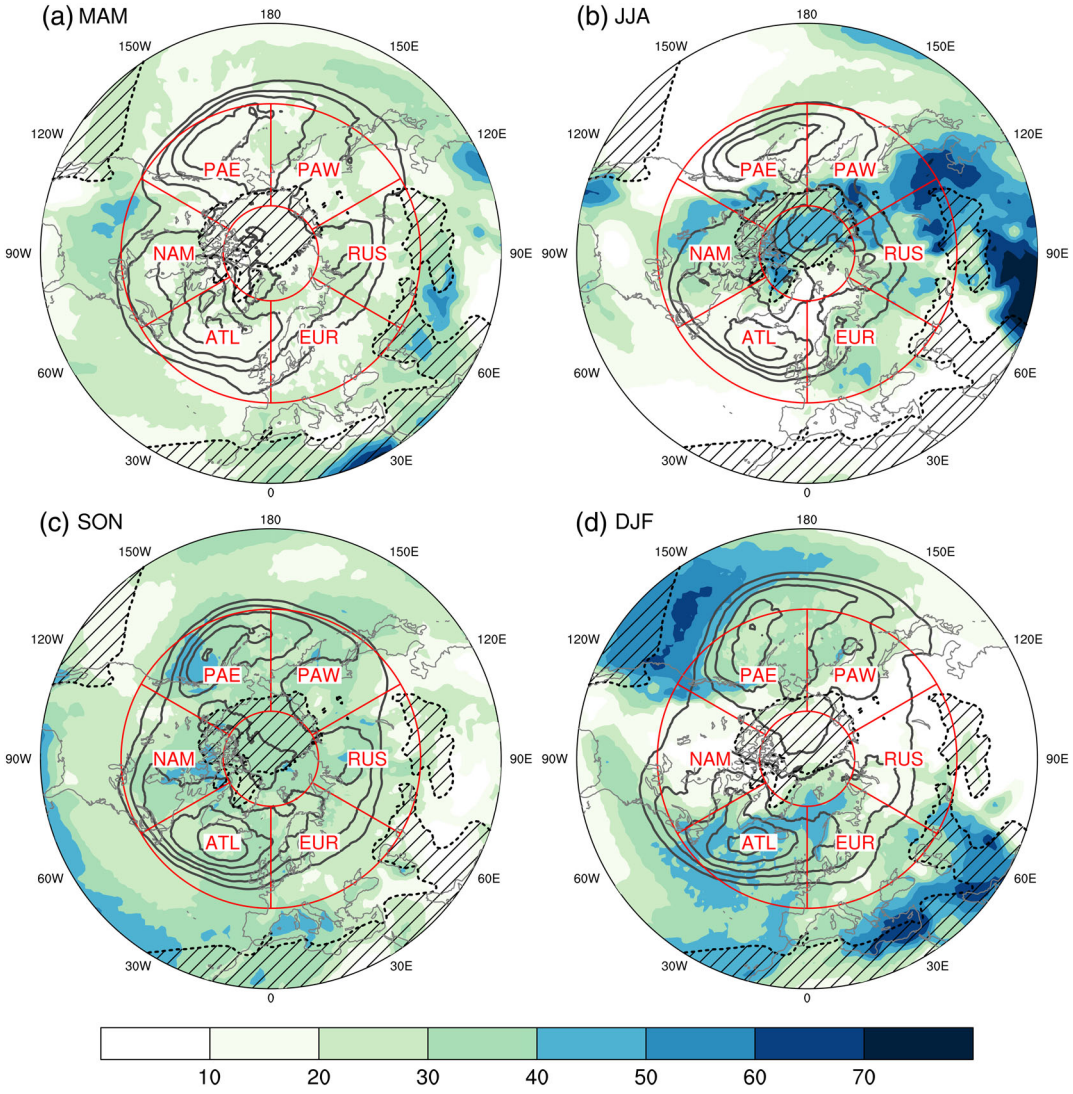

FIGURE 1 Seasonal distribution of daily precipitation events above the local all-year 95th precipitation percentile [%] (color shading). The values add up to 100% across the four seasons at every grid point. The solid black lines indicate the blocking frequency (in steps of 2%); the shaded areas indicate regions with a 95th yearly percentile of daily precipitation accumulation of less than 5 mm. The red boxes show the six different regions that were used in the analyses. Area mean 95th percentile values are PAW 10.1 mm, PAE 11.2 mm, NAM 9.2 mm, ATL 13 mm, EUR 9.2 mm, RUS 7.2 mm

2.2 | Atmospheric blocking, cyclone identification, and trajectory calculation

Following Schwierz *et al.* (2004) and Rohrer *et al.* (2018), atmospheric blocks are defined here as quasi-stationary upper tropospheric negative potential vorticity (PV) anomalies. Vertically averaged (500–150 hPa) 6-hourly PV anomaly fields were calculated with respect to the climatological 30-day running mean (1979–2015) and then smoothed with a 2-day running mean. All negative anomalies below a threshold of −1.3 PVU, with a persistence of 5 days or more, and a spatial overlap of at least 70% between adjacent time steps are identified as blocks. This results in binary fields of blocking presence or absence for every grid point and 6-hourly time step. From these binary fields, climatological blocking frequencies are computed, that is, the number of blocked time steps is divided by the total number of time steps. There is a strong seasonal cycle in the frequency of block occurrence (Figure 1). Blocks are the most frequent in DJF, with distinct spatial frequency maxima of 10–12% south of Greenland and over the east Pacific. Blocking frequencies are lowest in JJA. This seasonal cycle is partially due to the anomaly-based detection method. In summer the dynamical tropopause is higher and a very low PV anomaly is more difficult to achieve (Attinger *et al.*, 2019). However, a similar seasonal cycle is also found in blocking climatologies that are based on gradient reversal detection methods (Masato *et al.*, 2013).

Cyclones were identified using the automated detection method of Wernli *et al.* (2006) and Sprenger *et al.* (2017). This method results in binary fields of cyclone presence or absence for every grid point and 6-hourly time step of the ERA-Interim dataset. From these fields, seasonal cyclone frequencies were calculated in a manner analogous to the calculation of blocking frequencies.

All Northern Hemisphere blocks occurring in the years 2000–2004 were used as starting areas for 3-day back-trajectories. The trajectories were started every 6 hours from each latitude-longitude grid point in the blocks at five pressure levels (475, 400, 325, 250, and 175 hPa). Starting points with PV values of more than 2 PVU were removed from the analysis to exclude stratospheric air. A total of more than 27 million trajectories were calculated. The 3-day back-trajectories were calculated using the LAGRANTO2.0 tool (Wernli and Davies, 1997; Sprenger and Wernli, 2015). For every 6 hours between 0 and 72 hours, the position as well as several meteorological parameters (relative humidity, PV, potential temperature, total precipitation at the ground, and extreme precipitation at the ground) were traced along the trajectories. The number of trajectories per time step varies strongly over time, with a minimum value of 0 for time steps without blocks and a maximum value of 20160. To account for the latitudinal dependence of the grid cell area, the trajectories were weighted by the cosine of the latitude at the starting location.

2.3 | Trajectory selection and heating frequency

From all back-trajectories, those that were diabatically heated were selected as follows: air parcels undergoing a diabatic heating of more than 2 K (5 K) between the maximum potential temperature and the minimum at any earlier time step were labeled as moderately (strongly) diabatically heated following Pfahl *et al.* (2015). Note that the 5 K heating is weaker than the heating typically experienced by warm conveyor belt trajectories (Madonna *et al.*, 2014b).

To link diabatic heating to extreme precipitation, we followed the method of Lenggenhager *et al.* (2018). Air parcels passing over regions with extreme precipitation (daily precipitation above the local 95th all-year percentile) are assumed to be associated with precipitation at the ground if they are at least 80% saturated. A comparison with local diabatic heating rates and a visual investigation of the trajectories have shown that this threshold selects trajectories undergoing diabatic heating in the heavy precipitation area reasonably well (Lenggenhager *et al.*, 2019). The trajectories are split into six geographical regions of 60° longitude each according to their starting grid point (see Figure 1). The regions are the eastern Pacific (PAE; 180° W–120° W), North America (NAM; 120° W–60° W), the North Atlantic (ATL; 60° W–0° E), Europe (EUR; 0° E–60° E), Russia (RUS; 60° E–120° E), and the western Pacific (PAW; 120° E–180° E).

To identify the regions along the trajectories where diabatic heating is linked to heavy precipitation, 6-hourly binary gridded masks were created. Every grid point where a strongly heated backward trajectory (started from a block) passed heavy precipitation while being almost saturated (>80%) was recorded. Then, the mean of all time steps was calculated. This product is referred to as heavy precipitation-linked heating frequency.

3 | RESULTS AND DISCUSSION

3.1 | Fraction of diabatically heated air parcels in blocks

On average, 44% of all the trajectories were moderately heated (>2 K; not shown) in the 72 hours before they reached the block; 26% were strongly heated (>5 K; Figure 2a). This is in good agreement with the results of

Pfahl *et al.* (2015; 46% moderately heated in a 21-year climatology), Lenggenhager *et al.* (2018; 39% for October 2000), and Steinfeld and Pfahl (2019; 45% in a 38-year period). However, the fractions are highly variable in time. For individual time steps, the first and third quartiles of the fraction of trajectories that are moderately diabatically heated correspond to 30 and 56%, respectively (in accordance with Steinfeld and Pfahl, 2019, who found 33 and 55%). The first and third quartiles for the fraction of strongly diabatically heated air parcels correspond to 14 and 35%, respectively. A seasonal cycle is present in the fraction of diabatically heated trajectories. The median fraction of strongly heated air parcels is lowest in MAM and JJA (both 23%), slightly but significantly higher in SON (25%), and highest in DJF (27%) (Figure 2a).

The fraction of strongly heated air parcels also varies geographically (Figure 2b). In the European and Russian sectors (0° E–60° E and 60° E–120° E), the fraction of strongly diabatically heated air parcels is the smallest, with a median value of approximately 12%. In the American, Atlantic, and western Pacific sectors (120° W–60° W, 60° W–0° E, and 120° E–180° E), the median values are significantly higher and lie between 21 and 26%. The highest median value of 27% is found over the eastern Pacific sector (180° W–120°W). These results are in good agreement with those of Steinfeld and Pfahl (2019), who found moderately heated air parcels to be more prevalent over the oceans than over the continents.

3.2 | The role of heavy precipitation events in the diabatic heating of air parcels in blocks

Next, we link the strongly heated air parcels to heavy precipitation. Of all the trajectories that end in a block 19% pass a heavy precipitation area while being saturated. However,

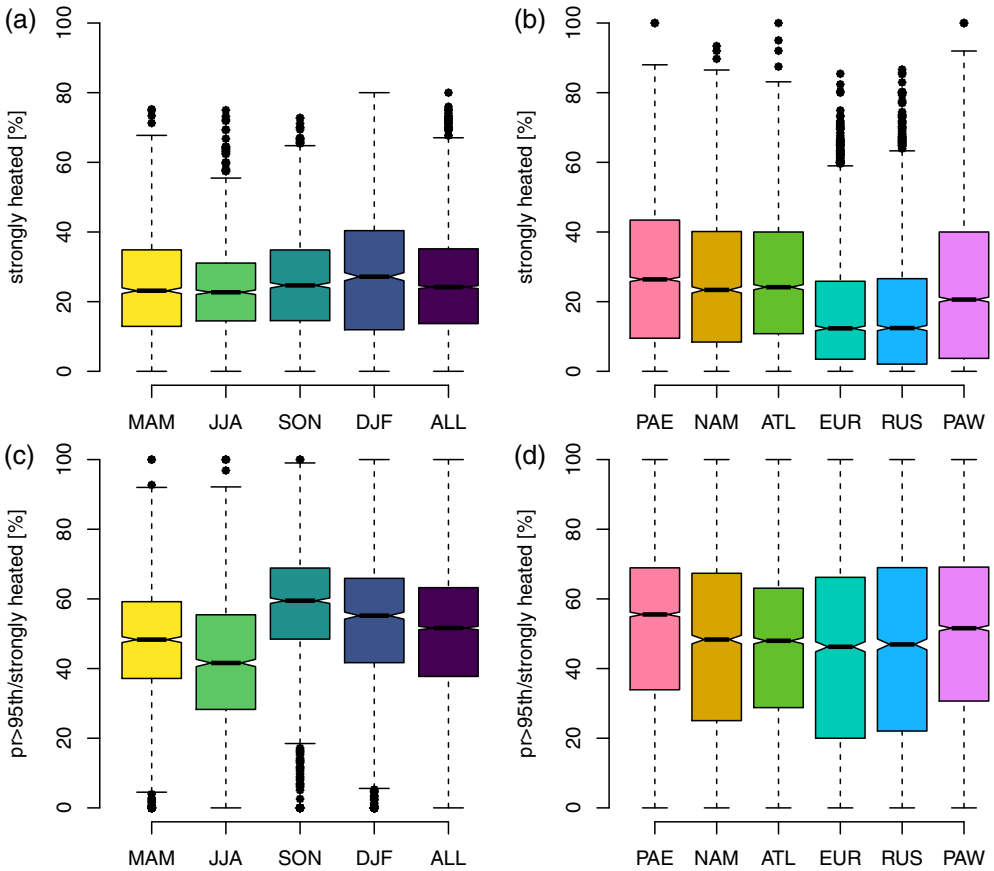

FIGURE 2 Seasonal (a, c) and regional (b, d) distribution of the fraction of strongly diabatically heated air (>5 K) arriving in the blocks (a, b) and the fraction of this strongly diabatically heated air that was associated with heavy precipitation above the 95th percentile (c, d). The median is indicated by the bold line. The notches of the boxplots around the median indicate the approximate 95% confidence interval for the median estimate calculated as $m \pm 1.58 \times (\text{interquartile range})/\sqrt{\text{sample}}$ (Krzywinski and Altman, 2014). If the notches of two boxes do not overlap, the medians differ significantly. The boxes indicate the interquartile range. The upper (lower) whiskers show either the third (first) quartile plus (minus) 1.5 times the interquartile range or the maximum value of the data if the latter is below this value. The lower whiskers show the first quartile minus 1.5 times the interquartile range or the maximum (minimum) value in the data if the latter is above this value. The smaller (larger) of the two values is shown

because we use a percentile-based definition of heavy precipitation the amount of precipitation varies regionally (Figure 1) and so does the associated heating. We therefore analyze which portion of the strongly heated air parcels pass through regions with heavy precipitation while being saturated. To answer this question, the fraction of air parcels that are heated in heavy precipitation regions and the total number of strongly diabatically heated air parcels are determined. On average, 54% of the strongly heated trajectories are associated with heavy precipitation.

The fraction of strongly diabatically heated air parcels that are associated with heavy precipitation events (Figure 2d) is more evenly distributed over the Northern Hemisphere than the fraction of all the strongly diabatically heated air (Figure 2b). Significant spatial differences are found only between the Pacific basin and the rest of the Northern Hemisphere. Between 120° W and 120° E, the median values lie between 46 and 48%. A significantly higher fraction is found over the Pacific, with a median of 52% over the western Pacific and a median of 56% over the eastern Pacific.

The fraction of all heated air parcels associated with heavy precipitation shows a pronounced seasonal cycle (Figure 2c). The highest median percentage of air parcels associated with daily precipitation above the 95th percentile is found in autumn (SON; 59%), followed by winter (DJF; 55%), spring (MAM; 48%), and summer (JJA; 42%). These fractions differ significantly from each other for all seasons (see notches in Figure 2c); the values of the upper quartiles also differ substantially between summer and autumn (Figure 2c). The seasonal cycle is generally less pronounced over the oceans than over the continents (Figure 3). Maximum values occur over the Pacific and the Atlantic in autumn (Figure 3a,c,f) and over North America, Europe, and Russia in winter. Over the North American (Figure 3b) and European (Figure 3d) sectors, there is a pronounced minimum in summer that is not present over the Pacific. The seasonal cycle is the most pronounced over the Russian sector (Figure 3e), with low values in spring and summer and very high values in fall and winter.

3.3 | Geographical location of heating related to heavy precipitation events

The geographic locations of air parcels that end up in blocks that are heated in areas of heavy precipitation,

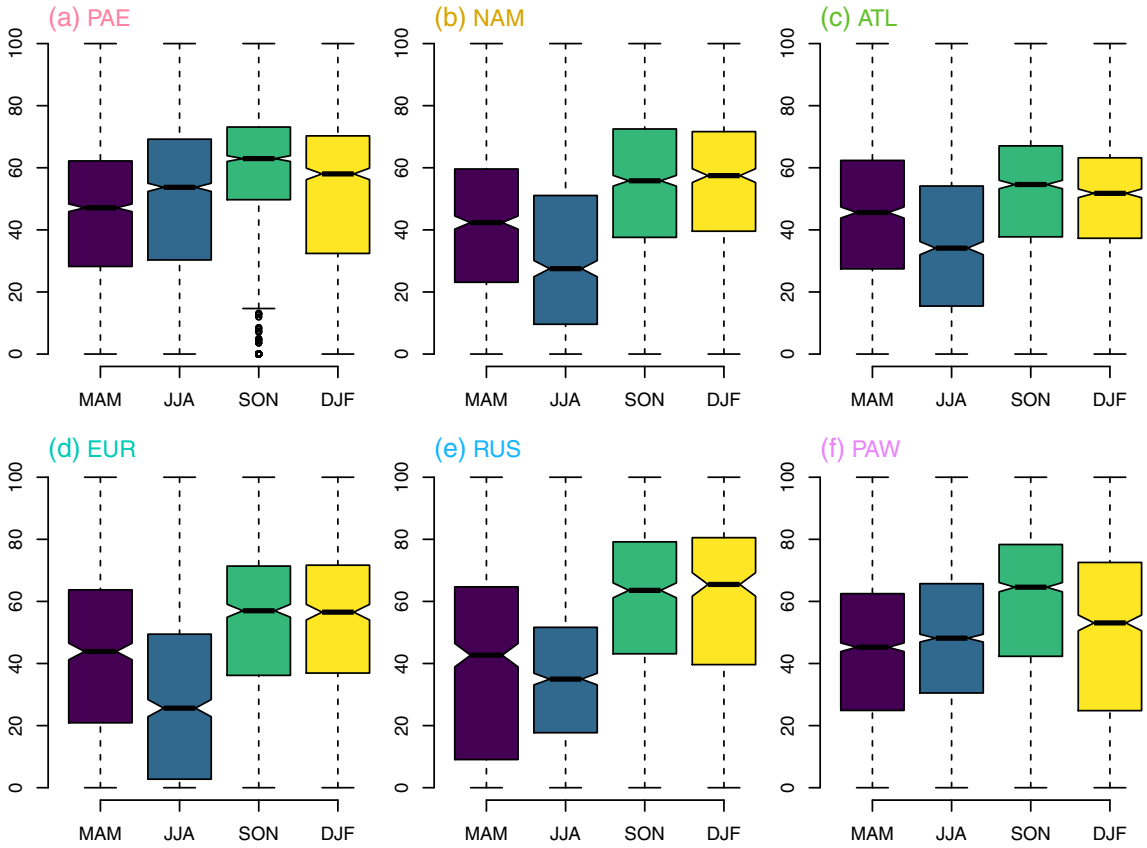

FIGURE 3 Seasonal distribution of the fraction of strongly diabatically heated air in the block, that was associated with heavy precipitation (>95th daily all-year percentile) for trajectories started in blocks in (a) the eastern Pacific (180° W–120° W), (b) North America (120° W–60° W), (c) Atlantic (60° W–0° E), (d) Europe (0° E–60° E), (e) Russia (60° E–120° E), and (f) western Pacific (120° E–180° E)

that is, where they are quasi-saturated, are illustrated in Figure 4. We show seasonal frequency, that is, the number of "heating" time steps divided by the overall number of time steps. The seasonal frequency of blocking is overlaid for orientation. The main regions where the strongly diabatically heated air parcels pass heavy precipitation areas are located over the North Atlantic and the Pacific (Figure 4). The maxima in the frequency of diabatically heated air parcels that end in blocks are located over the Pacific and the North Atlantic basin and are roughly colocated with parts of the storm tracks (approximated here by maxima in the cyclone frequency, see Figure 4). Over the Pacific, the percentage is highest over the west Pacific in MAM and JJA compared to SON and DJF, when a higher percentage is also present over the east Pacific. Over the North American continent, high percentage values are predominantly located in the eastern half of the storm tracks.

There are also strong seasonal variations in the distribution of the heating locations (Figure 4). In MAM (Figure 4a), the overall distribution of the heating frequencies is close to the annual mean frequencies (not shown). There is a strong maximum of up to 6% over the western Pacific region. Local values over the Eurasian continent are higher than the annual average and higher than at the same location in winter. In JJA (Figure 4b), the percentage values are generally much lower than in the other seasons, except for the Eurasian continent

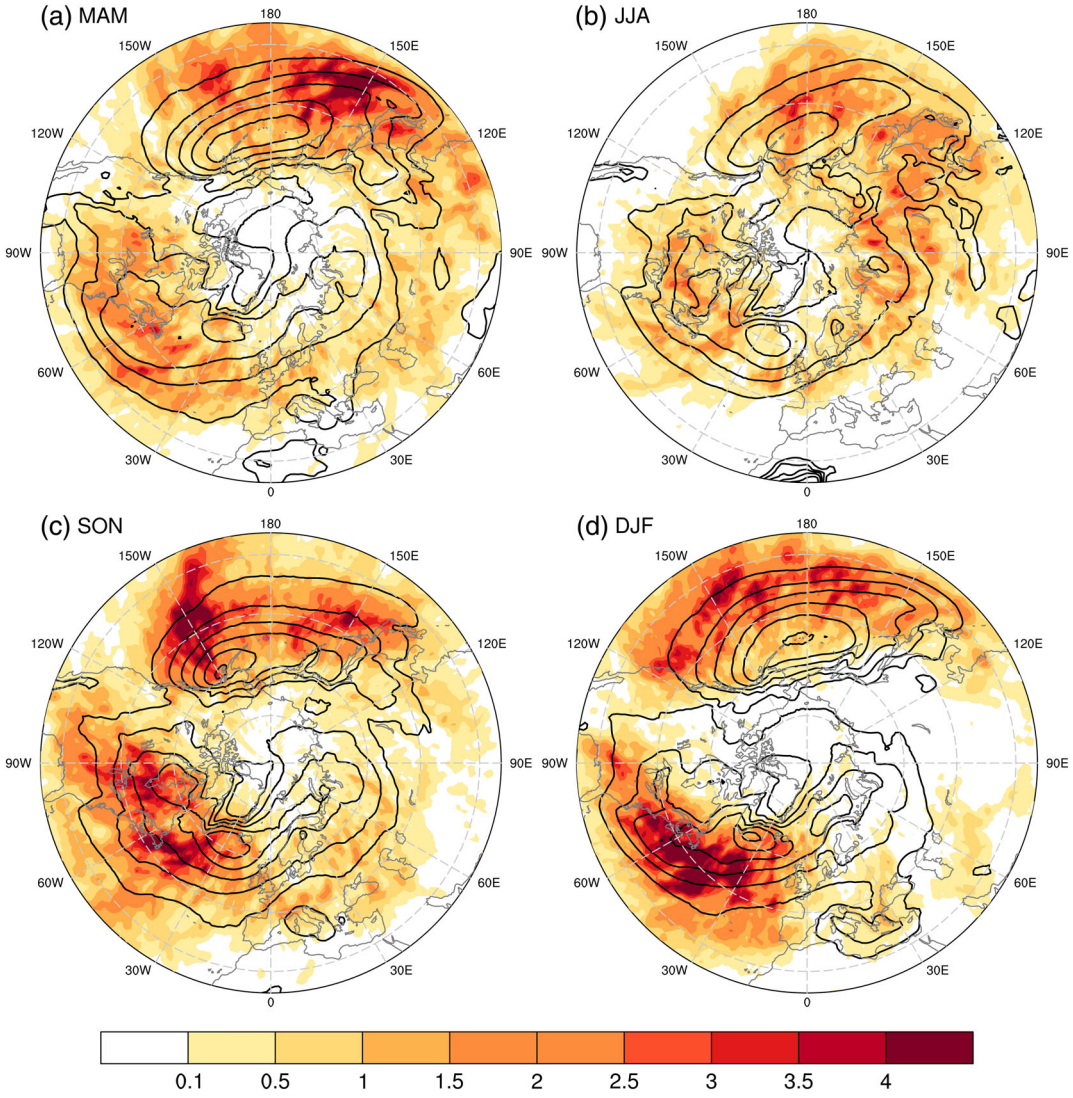

FIGURE 4 Seasonal fraction of 6-hourly time steps where strongly heated trajectories started from blocks were quasi-saturated and associated with daily precipitation above the 95th percentile (color shading, %). Note that values above 5% are possible due to the uneven seasonal distribution of days with precipitation above the 95th percentile (Figure 1) and that one trajectory may be counted multiple times. The location of heating associated with heavy precipitation is shown for (a) spring (MAM), (b) summer (JJA), (c) autumn (SON), and (d) winter (DJF). The solid black lines indicate the climatological cyclone frequency in 5% steps starting at 5%

where the highest frequencies of all seasons are found (up to 4%). In SON (Figure 4c), the highest frequencies are over the Pacific, eastern North America (highest frequencies of all seasons), and the western North Atlantic. In DJF (Figure 4d), the frequency maxima are over the Pacific, along the west coast of North America, and over the North Atlantic, where the highest frequency of all seasons are found with local maxima of 6%.

It is not straightforward to link the spatial patterns in Figure 4 to specific blocking regions, that is, to identify where trajectories that end up in a specific block were heated. We therefore illustrate this link for two regions in more detail by selecting all trajectories started from blocked grid points over the east Atlantic and Scandinavia (Figure 5; black boxes). The blocking frequency is higher in winter than in summer and higher over the central Atlantic than over Scandinavia. This seasonal difference in blocking frequency influences the absolute frequency values shown in Figure 5. This study therefore focuses on the comparison of the spatial patterns. For trajectories ending up in the central Atlantic blocks in summer, saturated air passes heavy precipitation areas primarily over the North American continent and over the western Atlantic, but also over Europe (upstream of the blocks; Figure 5a). In winter, the areas where the trajectories pass through heavy precipitation areas are located primarily over the western and central Atlantic (upstream and south of the blocks), the southeastern US, and the western Pacific (Figure 5c). The highest integral heating frequencies linked to local extreme precipitation are located approximately 30° upstream of the blocks. For trajectories ending up in the Scandinavian blocks in summer, saturated air passes local heavy precipitation areas primarily over the European continent and the

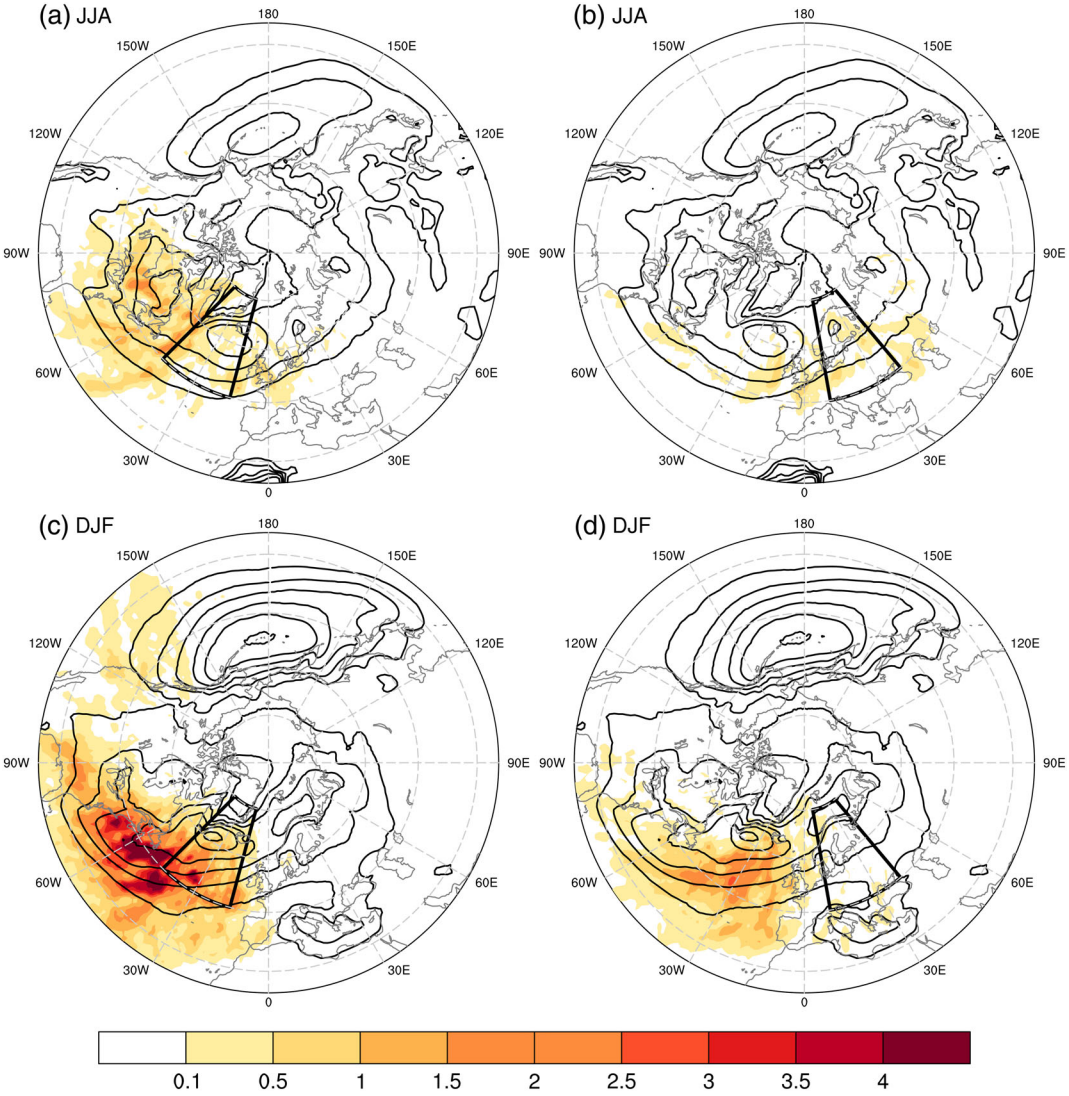

FIGURE 5 The same as Figure 4 but only for trajectories starting over the Central North Atlantic (a, c) and Europe (b, d) in summer (a, b) and winter (c, d)

north Atlantic. In winter, the areas where the trajectories pass through local heavy precipitation are located primarily over the central and eastern Atlantic. In addition, some trajectories pass through local heavy precipitation areas over the Mediterranean. The highest precipitation-linked heating densities are located roughly 60° upstream of the blocking area center.

4 | DISCUSSION

The spatial and seasonal variability in the fraction of diabatically heated trajectories and the fraction of heated trajectories that pass over heavy precipitation areas when saturated is strongly linked to the seasonality of both blocks and heavy precipitation events. Remember that all trajectories were started from blocks and are hence contingent on variations in seasonal blocking frequency. Generally, diabatically heated trajectories with heavy precipitation are strongly linked to the seasonality of the heavy precipitation events (compare Figures 1 and 4). Exceptions are the areas over the eastern US south of 40°N in autumn and the eastern Pacific in summer, where a relatively low percentage (20–30% and 10–30%, respectively) of heavy precipitation events influences blocks very efficiently.

The fraction of heated trajectories that pass through heavy precipitation shows a stronger seasonal cycle than the percentage of strongly heated air (Figure 2a,c). In winter, the frequency maxima are over the North Atlantic (Figure 4). This in contrast to all diabatically heated trajectories that are equally frequent over the North Atlantic and the Pacific (Pfahl *et al*., 2015).

The summer minimum in the link between heavy precipitation and strongly heated trajectories that reach blocks over the Atlantic and the continents (Figures 2c and 3) deserves some discussion since Pfahl *et al*. (2015) found more diabatically heated trajectories over the continents in summer than in winter (Figure 2a). In summer, the percentage of heavy precipitation events is high over northern North America, Europe, and eastern Asia and low over the Atlantic and Pacific (Figure 1). The summer minimum can hence be explained with two different hypotheses. First, if extreme precipitation in summer is generally more intensive, then precipitation events below the local 95th percentile are not captured with our methodology. However, these are still strong precipitation events and might therefore contribute strongly to diabatic PV modification. Second, if precipitation is generally weaker in summer, then the associated latent heat release is weaker and air parcels might not reach the upper troposphere and hence the blocks. The magnitude of the extreme precipitation, the seasonal distribution of precipitation extremes, and the locations where trajectories pass through heavy precipitation (Figures S1 and 4) do not confirm the first hypothesis but are compatible with the second. In addition, convective precipitation events in summer might be of shorter duration and higher intensity and therefore not captured by the 1-day accumulation extremes or not be resolved by the reanalysis data set.

The frequency maximum of heated trajectories that pass heavy precipitation areas over eastern North America in autumn could be partially linked to tropical cyclones undergoing extratropical transition (ET). The formation of strong ridges (blocks) downstream of ET cases is well documented (e.g., Grams *et al*., 2011; Keller *et al*., 2019; Pohorsky *et al*., 2019). The frequency maximum in winter could be partially linked to lee cyclones forming in this area (Wernli *et al*., 2006; Plante *et al*., 2015; Schultz *et al*., 2018; Bentley *et al*., 2019) and severe winter storms (e.g., Schultz *et al*., 2018; Bentley *et al*., 2019). Both the western Atlantic and the Scandinavian blocks contain low-PV air that passed heavy precipitation areas to the south or even to the east of the blocking sectors. This is partly related to the variability of the blocking location within the sectors. Since only the grid point from which the trajectory is started needs to be located inside the sector, blocks may extend upstream of the sectors. Omega blocks are associated with wave breaking and/or cut-off lows upstream and downstream of the blocking anticyclone (e.g., Altenhoff *et al*., 2008; Woollings *et al*., 2018). Thus, low PV air could also potentially enter blocks from upstream within the cyclonic circulation of a cut-off low located at the southeastern edge of a block. This hypothesis needs to be confirmed in further analyses.

The high contribution of heavy precipitation over land to the total number of strongly heated trajectories that pass over heavy precipitation events during the summer months (Figure 4b) is in accordance with the results of Steinfeld and Pfahl (2019), who found a high contribution of latent heating to summer blocks over Eurasia. This might point to a potentially indirect role of soil moisture in the formation of summer blocks via diabatic processes. That is, moisture that evaporates over land may contribute to heavy precipitation (Martius *et al*., 2013; Winschall *et al*., 2014) and hence to diabatic heating. This link could be explored further in the future.

A detailed evaluation of the processes that link heavy precipitation and blocks, for example, are blocks primarily supported through cross-isentropic PV transport or upper-level divergent flow (e.g., Grams and Archambault, 2016; Baumgart *et al*., 2018; Steinfeld and Pfahl, 2019) and the important link to discussions of adiabatic advection mechanisms (Wang and Kuang, 2019) should be addressed in future studies.

5 | CONCLUSIONS

This study demonstrates a link between heavy precipitation, associated latent heat release and air parcels ending up in Northern Hemisphere blocks. In total, 19% of the air parcels in blocks pass over heavy precipitation areas when saturated and more than half of the strongly diabatically heated air parcels (>5 K) that end up in blocks pass over regions with precipitation exceeding the local 95th all-year percentile. The fraction of heated air parcels that pass over heavy precipitation shows a strong seasonal cycle. The fraction is highest in winter (∼60%) and lowest in summer (∼40%). Note that the percentage values are dependent on the chosen heating and precipitation thresholds. We would expect the fraction to increase as the heating threshold increases. The fraction also varies between different geographical regions. The strongest relation is found for blocks over the Pacific (52–56%); elsewhere, the relation is weaker (46–48%) and lowest for the eastern European and Russian blocks.

The main regions where heated air parcels pass through heavy precipitation are located over the oceans, that is, the Pacific and the North Atlantic Ocean basins, and eastern North America in winter and over the Eurasian and American continents and the eastern Pacific in summer. For Scandinavian and North Atlantic blocks, the main heating regions associated with heavy precipitation are above the North Atlantic. In summer, the heating regions are located partly over the European continent; in winter, most air is heated upstream of the blocks (∼30° for Atlantic and ∼60° for Scandinavian blocks).

ACKNOWLEDGEMENTS

This study was funded by the Swiss National Science Foundation (grant number 156059). We would like to thank three anonymous reviewers for their constructive feedback that helped to substantially improve the quality of the paper.

ORCID

Sina Lenggenhager https://orcid.org/0000-0001-7398-8329

Olivia Martius https://orcid.org/0000-0002-8645-4702

REFERENCES

Altenhoff, A.M., Martius, O., Croci-maspoli, M., et al. (2008) Linkage of atmospheric blocks and synoptic-scale Rossby waves: a climatological analysis. *Tellus Series A: Dynamic Meteorology and Oceanography*, 60, 1053–1063. https://doi.org/10.1111/j.1600-0870.2008.00354.x.

Attinger, R., Keller, J.H., Köhler, M., Riboldi, J. and Grams, C.M. (2019) Representation of atmospheric blocking in the new global non-hydrostatic weather prediction model ICON. *Meteorologische Zeitschrift*, 28, 429–446. https://doi.org/10.1127/metz/2019/0967.

Baumgart, M., Riemer, M., Wirth, V., Teubler, F. and Lang, S.T.K. (2018) Potential vorticity dynamics of forecast errors: a quantitative case study. *Monthly Weather Review*, 146, 1405–1425. https://doi.org/10.1175/MWR-D-17-0196.1.

Bentley, A.M., Bosart, L.F. and Keyser, D. (2019) A climatology of extratropical cyclones leading to extreme weather events over central and eastern North America. *Monthly Weather Review*, 147, 1471–1490. https://doi.org/10.1175/MWR-D-18-0453.1.

Buehler, T., Raible, C.C. and Stocker, T.F. (2011) The relationship of winter season North Atlantic blocking frequencies to extreme cold or dry spells in the ERA-40. *Tellus Series A: Dynamic Meteorology and Oceanography*, 63, 212–222. https://doi.org/10.1111/j.1600-0870.2010.00492.x.

Chagnon, J.M., Gray, S.L. and Methven, J. (2013) Diabatic processes modifying potential vorticity in a North Atlantic cyclone. *Quarterly Journal of the Royal Meteorological Society*, 139, 1270–1282. https://doi.org/10.1002/qj.2037.

Croci-Maspoli, M. and Davies, H.C. (2009) Key dynamical features of the 2005/06 European winter. *Monthly Weather Review*, 137, 664–678. https://doi.org/10.1175/2008MWR2533.1.

Dee, D.P., Uppala, S.M., Simmons, A.J., Berrisford, P., Poli, P., Kobayashi, S., Andrae, U., Balmaseda, M.A., Balsamo, G., Bauer, P., Bechtold, P., Beljaars, A.C.M., van de Berg, L., Bidlot, J., Bormann, N., Delsol, C., Dragani, R., Fuentes, M., Geer, A.J., Haimberger, L., Healy, S.B., Hersbach, H., Hólm, E.V., Isaksen, L., Kållberg, P., Köhler, M., Matricardi, M., McNally, A.P., Monge-Sanz, B.M., Morcrette, J.J., Park, B.K., Peubey, C., de Rosnay, P., Tavolato, C., Thépaut, J.N. and Vitart, F. (2011) The ERA-Interim reanalysis: configuration and performance of the data assimilation system. *Quarterly Journal of the Royal Meteorological Society*, 137, 553–597. https://doi.org/10.1002/qj.828.

Grams, C.M. and Archambault, H.M. (2016) The key role of diabatic outflow in amplifying the midlatitude flow: a representative case study of weather systems surrounding Western North Pacific extratropical transition. *Monthly Weather Review*, 144, 3847–3869. https://doi.org/10.1175/MWR-D-15-0419.1.

Grams, C.M., Wernli, H., Böttcher, M., Čampa, J., Corsmeier, U., Jones, S.C., Keller, J.H., Lenz, C.J. and Wiegand, L. (2011) The key role of diabatic processes in modifying the upper-tropospheric wave guide: a North Atlantic case-study. *Quarterly Journal of the Royal Meteorological Society*, 137, 2174–2193. https://doi.org/10.1002/qj.891.

Gray, S.L., Dunning, C.M., Methven, J., Masato, G. and Chagnon, J.M. (2014) Systematic model forecast error in Rossby wave structure. *Geophysical Research Letters*, 41, 2979–2987. https://doi.org/10.1002/2014GL059282.

Hoskins, B.J., McIntyre, M.E. and Robertson, A.W. (1985) On the use and significance of isentropic potential vorticity maps. *Quarterly Journal of the Royal Meteorological Society*, 111, 877–946.

Illari, L. (1984) A diagnostic study of the potential vorticity in a warm blocking anticyclone. *Journal of the Atmospheric Sciences*, 41, 3518–3526. https://doi.org/10.1175/1520-0469(1984)041<3518:ADSOTP>2.0.CO;2.

Joos, H. and Wernli, H. (2012) Influence of microphysical processes on the potential vorticity development in a warm conveyor belt: a case-study with the limited-area model COSMO. *Quarterly Journal of the Royal Meteorological Society*, 138, 407–418. https://doi.org/10.1002/qj.934.

Keller, J.H., Grams, C.M., Riemer, M., Archambault, H.M., Bosart, L., Doyle, J.D., Evans, J.L., Galarneau, T.J., Jr., Griffin, K., Harr, P.A., Kitabatake, N., McTaggart-Cowan, R., Pantillon, F., Quinting, J.F., Reynolds, C.A., Ritchie, E.A., Torn, R.D. and Zhang, F. (2019) The extratropical transition of tropical cyclones. Part II: interaction with the midlatitude flow, downstream impacts, and implications for predictability. *Monthly Weather Review*, 147, 1077–1106. https://doi.org/10.1175/MWR-D-17-0329.1.

KrzywinskiMartin, Altman Naomi (2014) Visualizing samples with box plots. *Nature Methods*, 11, 119–120. http://dx.doi.org/10.1038/nmeth.2813.

Lenggenhager, S., Croci-Maspoli, M., Brönnimann, S. and Martius, O. (2019) On the dynamical coupling between atmospheric blocks and heavy precipitation events: a discussion of the southern alpine flood in October 2000. *Quarterly Journal of the Royal Meteorological Society*, 145, 530–545. https://doi.org/10.1002/qj.3449.

Lenggenhager, S. and Martius, O. (2019) Atmospheric blocks modulate the odds of heavy precipitation events in Europe. *Climate Dynamics*, 53, 4155–4171. https://doi.org/10.1007/s00382-019-04779-0.

Madonna, E., Limbach, S., Aebi, C., Joos, H., Wernli, H. and Martius, O. (2014a) On the co-occurrence of warm conveyor belt outflows and PV streamers. *Journal of the Atmospheric Sciences*, 71, 3668–3673. https://doi.org/10.1175/JAS-D-14-0119.1.

Madonna, E., Wernli, H., Joos, H. and Martius, O. (2014b) Warm conveyor belts in the ERA-Interim dataset (1979–2010). Part I: climatology and potential vorticity evolution. *Journal of Climate*, 27, 3–26. https://doi.org/10.1175/JCLI-D-12-00720.1.

Martius, O., Sodemann, H., Joos, H., Pfahl, S., Winschall, A., Croci-Maspoli, M., Graf, M., Madonna, E., Mueller, B., Schemm, S., Sedláček, J., Sprenger, M. and Wernli, H. (2013) The role of upper-level dynamics and surface processes for the Pakistan flood of July 2010. *Quarterly Journal of the Royal Meteorological Society*, 139, 1780–1797. https://doi.org/10.1002/qj.2082.

Masato, G., Hoskins, B.J. and Woollings, T. (2013) Winter and summer Northern Hemisphere blocking in CMIP5 models. *Journal of Climate*, 26, 7044–7059. https://doi.org/10.1175/JCLI-D-12-00466.1.

Massacand, A.C., Wernli, H., Davies, H.C., et al. (2001) Influence of upstream diabatic heating upon an alpine event of heavy precipitation. *Monthly Weather Review*, 129, 2822–2828. https://doi.org/10.1175/1520-0493(2001)129<2822:IOUDHU>2.0.CO;2.

Methven, J. (2015) Potential vorticity in warm conveyor belt outflow. *Quarterly Journal of the Royal Meteorological Society*, 141, 1065–1071. https://doi.org/10.1002/qj.2393.

Nakamura, H., Nakamura, M. and Anderson, J.L. (1997) The role of high- and low-frequency dynamics in blocking formation. *Monthly Weather Review*, 125, 2074–2093. https://doi.org/10.1175/1520-0493(1997)125<2074:TROHAL>2.0.CO;2.

Nakamura, N. and Huang, C.S.Y. (2018) Atmospheric blocking as a traffic jam in the jet stream. *Science*, 361, 42–47. https://doi.org/10.1126/science.aat0721.

Nakamura, N. and Huang, C.S.Y. (2017) Local wave activity and the onset of blocking along a potential vorticity front. *Journal of the Atmospheric Sciences*, 74, 2341–2362. https://doi.org/10.1175/JAS-D-17-0029.1.

Pfahl, S., Madonna, E., Boettcher, M., Joos, H. and Wernli, H. (2014) Warm conveyor belts in the ERA-Interim dataset (1979–2010). Part II: moisture origin and relevance for precipitation. *Journal of Climate*, 27, 27–40. https://doi.org/10.1175/JCLI-D-13-00223.1.

Pfahl, S., Schwierz, C., Croci-Maspoli, M., Grams, C.M. and Wernli, H. (2015) Importance of latent heat release in ascending air streams for atmospheric blocking. *Nature Geoscience*, 8, 610–614. https://doi.org/10.1038/ngeo2487.

Plante, M., Son, S.W., Atallah, E., Gyakum, J. and Grise, K. (2015) Extratropical cyclone climatology across eastern Canada. *International Journal of Climatology*, 35, 2759–2776. https://doi.org/10.1002/joc.4170.

Pohorsky, R., Röthlisberger, M., Grams, C.M., Riboldi, J. and Martius, O. (2019) The climatological impact of recurving North Atlantic tropical cyclones on downstream extreme precipitation events. *Monthly Weather Review*, 147, 1513–1532. https://doi.org/10.1175/MWR-D-18-0195.1.

Rex, D.F. (1950) Blocking action in the middle troposphere and its effect upon regional climate II. The climatology of blocking action. *Tellus*, 2, 275–301. https://doi.org/10.1111/j.2153-3490.1950.tb00339.x.

Rohrer, M., Brönnimann, S., Martius, O., Raible, C.C., Wild, M. and Compo, G.P. (2018) Representation of extratropical cyclones, blocking anticyclones, and alpine circulation types in multiple reanalyses and model simulations. *Journal of Climate*, 31, 3009–3031. https://doi.org/10.1175/JCLI-D-17-0350.1.

Schneidereit, A., Peters, D.H.W., Grams, C.M., Quinting, J.F., Keller, J.H., Wolf, G., Teubler, F., Riemer, M. and Martius, O. (2017) Enhanced tropospheric wave forcing of two anticyclones in the prephase of the January 2009 major stratospheric sudden warming event. *Monthly Weather Review*, 145, 1797–1815. https://doi.org/10.1175/MWR-D-16-0242.1.

Schultz, D.M., Bosart, L.F., Colle, B.A., Davies, H.C., Dearden, C., Keyser, D., Martius, O., Roebber, P.J., Steenburgh, W.J., Volkert, H. and Winters, A.C. (2018) Extratropical cyclones: a century of research on meteorology's centerpiece. *Meteorological Monographs*, 59, 16.1–16.56. https://doi.org/10.1175/amsmonographs-d-18-0015.1.

Schwierz, C., Croci-Maspoli, M. and Davies, H.C. (2004) Perspicacious indicators of atmospheric blocking. *Geophysical Research Letters*, 31, L06125. https://doi.org/10.1029/2003GL019341.

Shutts, G.J. (1983) The propagation of eddies in diffluent jetstreams: Eddy vorticity forcing of "blocking" flow fields. *Quarterly Journal of the Royal Meteorological Society*, 109, 737–761. https://doi.org/10.1002/qj.49710946204.

Sillmann, J., Mischa, C.M., Kallache, M. and Katz, R.W. (2011) Extreme cold winter temperatures in Europe under the influence of North Atlantic atmospheric blocking. *Journal of Climate*, 24, 5899–5913. https://doi.org/10.1175/2011JCLI4075.1.

Sousa, P.M., Trigo, R.M., Barriopedro, D., Soares, P.M.M., Ramos, A.M. and Liberato, M.L.R. (2017) Responses of European precipitation distributions and regimes to different blocking locations. *Climate Dynamics*, 48, 1141–1160. https://doi.org/10.1007/s00382-016-3132-5.

Sprenger, M., Fragkoulidis, G., Binder, H., Croci-Maspoli, M., Graf, P., Grams, C.M., Knippertz, P., Madonna, E., Schemm, S., Škerlak, B. and Wernli, H. (2017) Global climatologies of Eulerian and Lagrangian flow features based on ERA-Interim. *Bulletin of the American Meteorological Society*, 98, 1739–1748. https://doi.org/10.1175/BAMS-D-15-00299.1.

Sprenger, M. and Wernli, H. (2015) The LAGRANTO Lagrangian analysis tool—version 2.0. *Geoscientific Model Development*, 8, 2569–2586. https://doi.org/10.5194/gmd-8-2569-2015.

Steinfeld, D. and Pfahl, S. (2019) The role of latent heating in atmospheric blocking dynamics: a global climatology. *Climate Dynamics*, 53, 1–22. https://doi.org/10.1007/s00382-019-04919-6.

Teubler, F. and Riemer, M. (2016) Dynamics of Rossby wave packets in a quantitative potential vorticity–potential temperature framework. *Journal of the Atmospheric Sciences*, 73, 1063–1081. https://doi.org/10.1175/JAS-D-15-0162.1.

Wang, L. and Kuang, Z. (2019) Evidence against a general positive eddy feedback in atmospheric blocking. https://doi.org/10.31223/osf.io/kmgqv.

Wernli, H. and Davies, H.C. (1997) A Lagrangian-based analysis of extratropical cyclones 1. The method and some applications. *Quarterly Journal of the Royal Meteorological Society*, 123, 467–489. https://doi.org/10.1256/smsqj.53810.

Wernli, H., Schwierz, C., Wernli, H. and Schwierz, C. (2006) Surface cyclones in the ERA-40 dataset (1958–2001). Part I: novel identification method and global climatology. *Journal of the Atmospheric Sciences*, 63, 2486–2507. https://doi.org/10.1175/JAS3766.1.

Winschall, A., Pfahl, S., Sodemann, H. and Wernli, H. (2014) Comparison of Eulerian and Lagrangian moisture source diagnostics—the flood event in eastern Europe in May 2010. *Atmospheric Chemistry and Physics*, 14, 6605–6619. https://doi.org/10.5194/acp-14-6605-2014.

Woollings, T., Barriopedro, D., Methven, J., Son, S.W., Martius, O., Harvey, B., Sillmann, J., Lupo, A.R. and Seneviratne, S. (2018) Blocking and its response to climate change. *Current Climate Change Reports*, 4, 287–300. https://doi.org/10.1007/s40641-018-0108-z.

Yamazaki, A. and Itoh, H. (2013) Vortex-vortex interactions for the maintenance of blocking. Part I: the selective absorption mechanism and a case study. *Journal of the Atmospheric Sciences*, 70, 725–742. https://doi.org/10.1175/JAS-D-11-0295.1.

SUPPORTING INFORMATION

Additional supporting information may be found online in the Supporting Information section at the end of this article.

How to cite this article: Lenggenhager S, Martius O. Quantifying the link between heavy precipitation and Northern Hemisphere blocking—A Lagrangian analysis. *Atmos Sci Lett*. 2020;1–12. https://doi.org/10.1002/asl.999